Simultaneous control of pH and dissolved oxygen in closed photobioreactor

Mariana Titica
GEPEA, CNRS-UMR 6144
University of Nantes
Saint-Nazaire, France
Mariana.Titica@univ-nantes.fr

Antoinette Kazbar
GEPEA, CNRS-UMR 6144
University of Nantes
Saint-Nazaire, France
antoinette.kazbar@univ-nantes.fr

George Ifrim
Department of Automation and Electrical Engineering
Dunarea de Jos University
Galati, Romania
george.ifrim@ugal.ro

Helene Marec
GEPEA, CNRS-UMR 6144
University of Nantes
Saint-Nazaire, France
helene.marec@univ-nantes.fr

Jérémy Pruvost
GEPEA, CNRS-UMR 6144
University of Nantes
Saint-Nazaire, France
jeremy.pruvost@univ-nantes.fr

Marian Barbu
Department of Automation and Electrical Engineering
Dunarea de Jos University
Galati, Romania
marian.barbu@ugal.ro

Sergiu Caraman
Department of Automation and Electrical Engineering
Dunarea de Jos University
Galati, Romania
sergiu.caraman@ugal.ro

***Abstract*—This study investigates simultaneous pH and dissolved oxygen control (DO) in a closed photobioreactor (PBR), using a conventional linear feedback technique, i.e. individual PID and PID coupled with feedforward compensation. The proposed control scheme has been designed using linear approximations, whereas their evaluation has been done through simulation, considering a nonlinear process model, describing the complexity of this multivariable biological process. The proposed control including feedforward compensation present improved control performances, and consequently improves microorganism's growth conditions. This is of crucial importance in the case of lab scale set ups that have to provide fully controlled cultivation conditions for accurate study of growth dynamics.**

Keywords— microalgae, photobioreactor, dissolved oxygen controller, pH controller, feedback feed-forward scheme

I. INTRODUCTION

Today, the potential of microalgae is well established in a large number of applications, including food and cosmetics, but also third generation biofuels production, bio-mitigation of CO_2 and waste water treatment processes [1-6]. These photosynthetic microorganisms are able to transform solar energy into biomass, using as carbon source only CO_2 and mineral salts (nitrogen, phosphate), which can originate from gaseous and liquid waste effluents, respectively. At the same time, they produce O_2 through photosynthesis, which argued in favor of coupling with aerobic bioprocesses, as for example, activated sludge [6].

To be competitive and sustainable, processes using microalgae have to meet some specific requirements, which justify important research effort on system cultivation technologies. A wide variety exists, from extensive open (raceway) and closed system, to intensified technologies, enabling very thin culture depth with high specific illuminated area [7]. Efficient operation, for maintaining optimum operating conditions, despite fluctuating environment (especially in outdoor cultivation) is mandatory to ensure high biomass productivities expected by the design [8].

The cultivation system (called photobioreactor, PBR) is a complex process influenced by multiple parameters, such as photosynthetic light capture and attenuation, nutrient uptake, PBR hydrodynamics and gas – liquid (G – L) mass transfer. From a control perspective, the variables to be controlled in a photobioreactor can be classified in two categories: physicochemical, related to the culture medium (pH, temperature, mineral nutrients, dissolved gases (O_2, CO_2, light gradient inside the broth), and biological (cells and metabolite concentrations and biological activity).

Various control technics, most of them model based, have been reported in the literature (e.g. optimal control, predictive control, adaptive control and feedback linearization) to control cell concentration in a photobioreactor, considering light as only limiting factor of growth [9 - 12]. But photosynthetic response of the microalgae with respect to light strongly depends on physicochemical variables that must be properly handled with appropriate control technics. pH control scheme has been proposed in the literature [12-14]. The simultaneous control of dissolved oxygen and pH have been less considered; a selective control scheme within an event-based approach has been proposed for a pilot scale raceway [15].

In this paper, we consider the pH and dissolved oxygen concentration control. Their behavior in a PBR is highly dynamic because is influenced by the photosynthetic rate, and hence they must be kept closed to their optimal values.

The paper is organized as follows: first two sections are dedicated to the process description and the formulation of the

control problem. Then, the nonlinear model used here as a virtual plant of a closed photobioreactor system has been briefly introduced. Section 3 presents the design of the control scheme. Results are presented in Section 4, before concluding.

II. Process Description and Control Problem Formulation

A. Process description

During phototrophic growth, microalgae consume carbon dioxide (CO_2) and produce oxygen (O_2). The inorganic carbon (CO_2) is supplied in gaseous form to provide the sufficient dissolved inorganic carbon avoiding photosynthesis growth limitations. CO_2 dissolution is accompanied with a pH decrease, while bicarbonate consumption by microalgae during photosynthesis causes pH increase. Consequently, the CO_2 injection is used for pH control purposes.

The oxygen evolved during the photosynthetic growth can easily build up to high concentrations in closed photobioreactors (PBRs) and this can have a negative effect on biomass productivity by inhibiting the growth of the microalgae cells [16 – 18]. In day/night cycles, for example, photosynthetic growth depends on the photon flux density, that could reach high levels. In the same manner, production of photosynthetic oxygen by microalgae cells varies throughout the day and could attain concentrations that might cause photosynthetic apparatus damage. Regulation of dissolved oxygen concentrations in the culture systems is thus required. The excessive concentration of dissolved oxygen could be avoided by an effective gas stripping that can evacuate oxygen from the system. Gas stripping causes also CO_2 desorption (from the liquid to the gaseous phase), causing an increase in pH, and thus interfering with the pH regulation loop.

Different configurations exist for CO_2 supply and air striping in the PBR. It depends on the technology and considered application. The process considered here, concerns a pilot scale photobioreactor. It is a torus-shaped PBR that has been designed for lab-scale experiments requiring a tight control of culture conditions. One of its main feature is to allow varying gas-liquid mass transfer efficiency in a wide extend; in fact, culture is mechanically circulated thanks to the rotation of a marine impeller and to air (or nitrogen) bubbling. As mixing is mainly provided by mechanical stirring, this was found valuable for studies requiring accurate gas analysis [19]. If necessary, gas bubbling could obviously be applied, so as to increase the gas-liquid mass transfer rate. Because of the accurate control of culture conditions, the torus photobioreactor has been used widely in recent years for in-depth studies and kinetic model and control settings [12, 20, 21]. The torus PBR with associated instrumentation and control settings is fully described elsewhere [12, 19]. A schematic representation is given in Fig. 1.

B. Control problem definition

The control objective is to simultaneously control the dissolved oxygen, below the inhibition level (25 mg/L observed experimentally), and the pH around its optimal value (7.5 for *Chlamydomonas reinhardtii*). Two manipulated variables could be used for this purpose: pure CO_2 injection flowrate and nitrogen injection flowrates. Dilution rate and incident light represents main disturbances because they influence photosynthetic growth rate.

The dissolved oxygen can be controlled based on the stripping effect on N_2 gas. Increasing the N_2 gas flowrate, the dissolved oxygen produced through photosynthesis will decrease. The pH is conventionally control by bubbling CO_2 gas in the culture, which is also a source of carbon for microalgae growth (inorganic carbon).

The stripping effect of N_2 gas is not limited to the dissolved oxygen, but also to the dissolved CO_2. Stripping more dissolved oxygen will result in stripping more dissolved CO_2, the pH will increase, and the pH controller must compensate rapidly the loss. It results thus in a multivariable system with strong interactions between the channels.

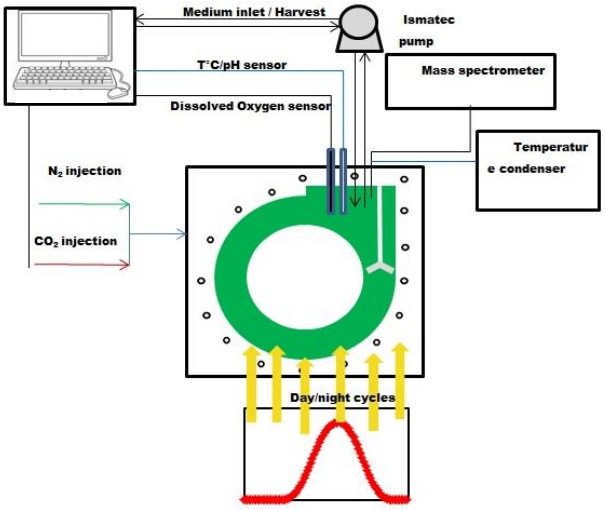

Fig. 1. Schematic representation of the photobioreactor

The objective is to evaluate the degree of interaction between the two I/O channels and to investigate for decoupling solutions.

III. Modeling and System Analysis

A. Modeling of photosynthetic growth process

A model based on first principles was used to appreciate the complexity of this multivariable biological process [22] The global phototrophic growth model used for simulation was presented extensively in [20]. A brief description is given here. To express the evolution of the pH, the model accounts all chemical species of the ternary solute system $NH_3 - CO_2 - H_2O$. The model results in a high order DAE system (the last 11 states are algebraic equations treated as differential equations with fast dynamics). The global photoautotrophic growth was obtained through the association of three sub-models: a radiative model, a biological model and a thermodynamic model. The radiative transfer (Eq. 1) model

describes the attenuation of light inside the culture of microalgae:

$$G(z) = q_0 e^{-\frac{1+\alpha}{2\alpha}E_a X z} \quad (1)$$

with $\alpha = \sqrt{(E_a)/(E_a + 2bE_s)}$. G - irradiance, z - depth of the culture, q_0 – incident light intensity, E_a and E_s - the mass absorption and the mass scattering coefficients, b - the backward scattering fraction (dimensionless), X - biomass concentration. The coupling between the radiative model and the biological model (Eq. 2) was made through the global volumetric growth rate, r_x,

$$\langle r_x \rangle = (\mu_G - \mu_s)X = \left(\mu_{max} \int_0^L \frac{G(z)}{K_I + G(z)} dz - \mu_s\right) X \quad (2)$$

where μ_G is the specific growth rate related to photosynthesis, μ_s is the specific respiration rate, μ_{max} is the maximum specific growth rate, K_I the half-saturation constant and L is the depth of the photobioreactor.

The biological sub-model describes the dynamics of 8 states: biomass, X, total inorganic nitrogen, TIN, total inorganic carbon, TIC, dissolved oxygen, $c_{\mathrm{CO_2}}$, output molar fractions of CO_2, O_2 and N_2, $y_{out}^{\mathrm{CO_2}}$, $y_{out}^{\mathrm{O_2}}$ and $y_{out}^{\mathrm{N_2}}$, and the total output gas, G_{out}.

The volumetric rates for TIN, TIC and $c_{\mathrm{CO_2}}$ are expressed as functions of r_x (Eqs. 3):

$$\langle r_{\mathrm{TIN}} \rangle = \frac{Y_{N/X}}{M_x}\langle r_x \rangle;\ \langle r_{\mathrm{TIC}} \rangle = \frac{1}{M_x}\langle r_x \rangle;\ \langle r_{O_2} \rangle = \frac{Q_P}{M_x}\langle r_x \rangle \quad (3)$$

where M_x is the C-mole mass, $Y_{N/X}$ is the yield of TIN conversion and Q_P is the photosynthetic quotient.

The volumetric G-L mass transfer rates for O_2 and CO_2, $N_{\mathrm{O_2}}$ and $N_{\mathrm{CO_2}}$, are modeled using the two-film theory:

$$N_{\mathrm{O_2}} = (K_L a)_{\mathrm{O_2}} \left(\frac{y_{\mathrm{O_2}}^{\mathrm{lm}} P}{H_{\mathrm{O_2}}} - c_{\mathrm{O_2}}\right) \quad (4)$$

$$N_{\mathrm{CO_2}} = (K_L a)_{\mathrm{CO_2}} \left(\frac{y_{\mathrm{CO_2}}^{\mathrm{lm}} P}{\gamma_{\mathrm{CO_2}} H_{\mathrm{CO_2}}} - c_{\mathrm{CO_2}}\right) \quad (5)$$

The overall volumetric mass-transfer coefficient for oxygen was identified on experimental data:

$$(K_L a)_{\mathrm{O_2}} = 1.1806 * (Q_e/V_l)^{0.7610} \quad (6)$$

where $Q_e = Q_{in}^{\mathrm{CO_2}} + Q_{in}^{\mathrm{N_2}}$, the sum of the feeding CO_2 and N_2 gas flow rates expressed in mL/min ($G_{in}^{\mathrm{CO_2}}$ and $G_{in}^{\mathrm{N_2}}$ are the same measurements expressed in mol/h). $(K_L a)_{\mathrm{CO_2}}$ is determined from the molecular diffusivities of CO_2 and O_2: $(K_L a)_{\mathrm{CO_2}} = (K_L a)_{\mathrm{O_2}} (D_{\mathrm{CO_2}}/D_{\mathrm{O_2}})$.

The thermodynamic model describes the dynamics of all chemical species of the ternary solute system and the pH: dissolved carbon dioxide, $c_{\mathrm{CO_2}}$, bicarbonate ions, $c_{\mathrm{HCO_3^-}}$, carbonate ions, $c_{\mathrm{CO_3^{2-}}}$, carbamate ions, $c_{\mathrm{NH_2COO^-}}$, ammonia, $c_{\mathrm{NH_3}}$, ammonium ions, $c_{\mathrm{NH_4^+}}$, hydroxyl ions, $c_{\mathrm{OH^-}}$, and hydrogen ions, $c_{\mathrm{H^+}}$.

The global photoautotrophic growth model is presented in state-space form in Eq. 7. The model was developed to be used also for continuous processes when the dilution rate, D represents the rate of nutrient exchange (the ratio between the liquid flowrate and the culture volume). In the transport terms, $c_{\mathrm{TIN},i}$ and $c_{\mathrm{TIC},i}$ are the concentrations of TIN and TIC in the feed.

$$\begin{cases} \dot{x} = \begin{bmatrix} \dot{X} \\ \dot{c}_{\mathrm{TIN}} \\ \dot{c}_{\mathrm{TIC}} \\ \dot{c}_{\mathrm{O_2}} \\ \dot{y}_{out}^{\mathrm{CO_2}} \\ \dot{y}_{out}^{\mathrm{O_2}} \\ \dot{y}_{out}^{\mathrm{N_2}} \\ \dot{G}_{out} \\ \dot{c}_{\mathrm{CO_2}} \\ \dot{c}_{\mathrm{HCO_3^-}} \\ \dot{c}_{\mathrm{CO_3^{2-}}} \\ \dot{c}_{\mathrm{NH_2COO^-}} \\ \dot{c}_{\mathrm{NH_3}} \\ \dot{c}_{\mathrm{NH_4^+}} \\ \dot{c}_{\mathrm{OH^-}} \\ \dot{c}_{\mathrm{H^+}} \\ \dot{\mathrm{pH}} \end{bmatrix} = \begin{bmatrix} \langle r_x \rangle - DX \\ -\langle r_{\mathrm{TIN}} \rangle + D(c_{\mathrm{TIN},i} - c_{\mathrm{TIN}}) \\ -\langle r_{\mathrm{TIC}} \rangle + D(c_{\mathrm{TIC},i} - c_{\mathrm{TIC}}) + N_{\mathrm{CO_2}} \\ \langle r_{\mathrm{O_2}} \rangle - D c_{\mathrm{O_2}} + N_{\mathrm{O_2}} \\ RT/PV_g \left(-y_{out}^{\mathrm{CO_2}} G_{out} - V_l N_{\mathrm{CO_2}}\right) \\ RT/PV_g \left(G_{in}^{\mathrm{O_2}} - y_{out}^{\mathrm{O_2}} G_{out} - V_l N_{\mathrm{O_2}}\right) \\ y_{out}^{\mathrm{CO_2}} + y_{out}^{\mathrm{O_2}} + y_{out}^{\mathrm{N_2}} - 1 \\ 0 \\ c_{\mathrm{TIC}} - c_{\mathrm{HCO_3^-}} - c_{\mathrm{CO_3^{2-}}} - c_{\mathrm{NH_2COO^-}} - c_{\mathrm{CO_2}} \\ K_1 \gamma_{\mathrm{CO_2}} c_{\mathrm{CO_2}} a_w / (\gamma_{\mathrm{HCO_3^-}} \gamma_{\mathrm{H^+}} c_{\mathrm{H^+}}) - c_{\mathrm{HCO_3^-}} \\ K_2 \gamma_{\mathrm{HCO_3^-}} c_{\mathrm{HCO_3^-}} / (\gamma_{\mathrm{CO_3^{2-}}} \gamma_{\mathrm{H^+}} c_{\mathrm{H^+}}) - c_{\mathrm{CO_3^{2-}}} \\ \gamma_{\mathrm{NH_3}} c_{\mathrm{NH_3}} \gamma_{\mathrm{HCO_3^-}} c_{\mathrm{HCO_3^-}} / (K_4 \gamma_{\mathrm{NH_2COO^-}} a_w) - c_{\mathrm{NH_2COO^-}} \\ c_{\mathrm{TIN}} - c_{\mathrm{NH_4^+}} - c_{\mathrm{NH_2COO^-}} - c_{\mathrm{NH_3}} \\ K_3 \gamma_{\mathrm{NH_3}} c_{\mathrm{NH_3}} a_w / (\gamma_{\mathrm{NH_4^+}} \gamma_{\mathrm{OH^-}} c_{\mathrm{OH^-}}) - c_{\mathrm{NH_4^+}} \\ K_w a_w / (\gamma_{\mathrm{OH^-}} \gamma_{\mathrm{H^+}} c_{\mathrm{H^+}}) - c_{\mathrm{OH^-}} \\ c_{\mathrm{HCO_3^-}} + 2c_{\mathrm{CO_3^{2-}}} + c_{\mathrm{NH_2COO^-}} + c_{\mathrm{OH^-}} - c_{\mathrm{NH_4^+}} + ct - c_{\mathrm{H^+}} \\ -log(\gamma_{\mathrm{H^+}} c_{\mathrm{H^+}}) - \mathrm{pH} \end{bmatrix} + \begin{bmatrix} 0 \\ 0 \\ 0 \\ 0 \\ 0 \\ 0 \\ 0 \\ 1/y_{out}^{\mathrm{O_2}} \\ 0 \\ 0 \\ 0 \\ 0 \\ 0 \\ 0 \\ 0 \\ 0 \\ 0 \\ 0 \end{bmatrix} G_{in}^{\mathrm{N_2}} + \begin{bmatrix} 0 \\ 0 \\ 0 \\ 0 \\ 0 \\ RT/PV_g \\ 0 \\ 0 \\ 0 \\ 0 \\ 0 \\ 0 \\ 0 \\ 0 \\ 0 \\ 0 \\ 0 \\ 0 \end{bmatrix} G_{in}^{\mathrm{CO_2}} \\ y_1 = c_{\mathrm{O_2}} \\ y_2 = \mathrm{pH} \end{cases} \quad (7)$$

As described above, the photosynthetic growth of microalgae is influenced by the pH and the dissolved oxygen and therefore functions normalized between 0 and 1, that describe their effect have been introduced. Eq. 2 was thus modified as follows:

$$\langle r_x \rangle = \left(\mu_G f_{pH} f_{DO} - \mu_s\right) X \tag{8}$$

The influence of pH on the photosynthesis rate has expressed using a parabolic like function, with the maximum at 7.5 (as reported into the literature) (Eq. 9).

$$f_{\mathrm{pH}} = \frac{\mathrm{pH}-\mathrm{pH}_{\min}}{\mathrm{pH}_{\max}-\mathrm{pH}} e^{\left(1-\frac{\mathrm{pH}-\mathrm{pH}_{\min}}{\mathrm{pH}_{\max}-\mathrm{pH}}\right)} \tag{9}$$

where $\mathrm{pH}_{\min}$ and $\mathrm{pH}_{\max}$ are the values of the pH below/above which no photosynthetic grow is observed (these values have been fixed at 4 and 11, respectively).

It was observed experimentally on *Chlamydomonas reinhardtii* cultures that the DO concentration became influent for concentrations higher than 25 mg/L (~300%). About 20% decrease in productivity was estimated in the presence of higher levels of DO, around 40 mg/L (500%). This DO level has been observed, when the incident light was at 800 µmol/m^2/s. To take into consideration dissolved oxygen influence, following function has been used:

$$f_{\mathrm{DO}} = \frac{1}{1+10^{-23}{c_{\mathrm{O}_2}}^{14}} \tag{10}$$

Fig. 2 shows the pH and DO inhibition functions that penalize the specific grow rate (Eq. 8).

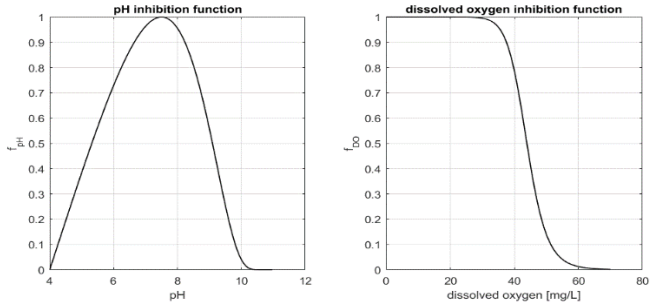

Fig. 2 pH and DO inhibition functions

The parameters of the global photoautotrophic growth model can be found in [20].

B. The RGA Analysis

To evaluate the simultaneous control of the dissolved oxygen and the pH an RGA analysis was employed. The RGA analysis, developed by Bristol in 1966 [23], is a steady-state measure that quantifies the degree of interaction between I/O signals. The RGA was defined initially for a $n \times n$ square system. The elements of the array, λ_{ij} (i.e. relative gains), are the gain of an element $[H(s)]_{ij}$ in the transfer matrix $H(s)$ when all the other loops are open, and the gain of the same element when all the other loops are perfectly controlled. The RGA of a non-singular square matrix $H(s)$ is a square matrix frequently computed as:

$$\mathrm{RGA}(H) = \Lambda(H) \triangleq H(s) \times \left(H(s)^{-1}\right)^T \tag{11}$$

where $\times$ denotes element-by-element multiplication (Schur product). The Laplace-variable s is 0 for steady-state systems.

The RGA has several algebraic and control properties that makes it attractive for evaluating the multivariable systems in terms of degree of interaction between the control channels and pairing suggestions for decentralized control. From an algebraic viewpoint the RGA is independent of input and output scaling and its rows and columns sum is equal to one: $\sum_{i=1}^{m} \lambda_{ij} = \sum_{j=1}^{m} \lambda_{ij} = 1$.

The RGA for a 2×2 steady-state system, $H = \begin{bmatrix} h_{11} & h_{12} \\ h_{21} & h_{22} \end{bmatrix}$, is:

$$\Lambda(H) = \begin{bmatrix} \lambda_{11} & \lambda_{12} \\ \lambda_{21} & \lambda_{22} \end{bmatrix} = \begin{bmatrix} \lambda_{11} & 1-\lambda_{11} \\ 1-\lambda_{11} & \lambda_{11} \end{bmatrix} \tag{12}$$

where $\lambda_{11} = 1/(1-\kappa)$, with $\kappa \triangleq (h_{12}h_{21})/(h_{11}h_{22})$. κ represents the interaction measure.

From a control point of view, the system can be decoupled if λ_{11} is close to 1. In this case the interaction with other loops ($u_j \rightarrow y_{i,\forall i \neq j}$) is minimal and the pairing may be done along the diagonal. On the contrary, $0 < \lambda_{11} < 1$ denotes interactions and the decentralized control can be ineffective.

Given that the objective is to control the dissolved oxygen, assumed to inhibit the growth of microalgae above 25 mg/L, and the pH, whose optimal value is 7.5, it results a 2×2 square system as presented in Fig. 3.

The control variables are the feeding CO_2 and N_2 gas flow rates, $Q_{in}^{\mathrm{CO}_2}$ and $Q_{in}^{\mathrm{N}_2}$, respectively. $Q_{in}^{\mathrm{CO}_2}$ interferes with the TIC system and decreases the pH when it is bubbled into the culture. The $Q_{in}^{\mathrm{N}_2}$ has a stripping effect over the dissolved oxygen, c_{O_2}, lowering its concentration inside the microalgae culture. However, $Q_{in}^{\mathrm{N}_2}$ will strip out at the same time the dissolved CO_2 and will interfere with the pH regulation loop ($Q_{in}^{\mathrm{CO}_2} \rightarrow \mathrm{pH}$).

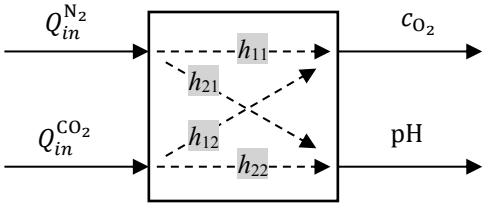

Fig. 3. The square system of the PBR

$Q_{in}^{\mathrm{CO}_2}$ and $Q_{in}^{\mathrm{N}_2}$ are expressed in mL/min, while $G_{in}^{\mathrm{CO}_2}$ and $G_{in}^{\mathrm{N}_2}$ are expressed in mol/h. The first ones are preferred here because they are the actual measuring unit the CO_2 and N_2 gas flow meters. The CO_2 flow meter provided for the torus-shaped PBR has a maximum flow rate of 10 mL/min while the N_2 flow meter, a maximum flow rate of 100 mL/min. These upper bounds will be used to saturate the control variables. The conversion between $Q_{in}^{\mathrm{CO}_2}$ (mL/min) and $G_{in}^{\mathrm{CO}_2}$ (mol/h) can be done by using the ideal gas law (and the same for N_2):

$$Q_{in}^{\mathrm{CO}_2} = \frac{R \cdot T \cdot G_{in}^{\mathrm{CO}_2} \cdot 10^6}{P \cdot 60} \tag{13}$$

By means of the fully functional global photoautotrophic growth model presented above, that is able to express the stripping effect of N_2 over O_2 and CO_2, the degree of interaction between the two channels can be evaluated through an RGA analysis. The following square system will be used for the RGA analysis:

$$\begin{bmatrix} c_{O_2} \\ \text{pH} \end{bmatrix} = \begin{bmatrix} H_{G_{in}^{N_2}-c_{O_2}} & H_{G_{in}^{CO_2}-c_{O_2}} \\ H_{G_{in}^{N_2}-\text{pH}} & H_{G_{in}^{CO_2}-\text{pH}} \end{bmatrix} \begin{bmatrix} G_{in}^{N_2} \\ G_{in}^{CO_2} \end{bmatrix} \quad (14)$$

For the RGA analysis the dilution was considered constant (D = 0.04 h^{-1} – optimal dilution in terms of biomass productivity [12]) and also the incident light intensity (q_0 = 300 µmol/m^2/s, commonly used in laboratory experiments under artificial light).

The combination of gas flows $Q_{in}^{N_2}$ = 20 mL/min and $Q_{in}^{CO_2}$ = 1.3 mL/min, that lead to a pH of app. 7.5 and c_{O_2} = 27.2 mg/L, presents low cross-interactions that suggests decentralized control.

$$\Lambda_{c_{O_2}=27.2}^{\text{pH}=7.5} = \begin{bmatrix} 0.9944 & 0.0056 \\ 0.0056 & 0.9944 \end{bmatrix} \quad (15)$$

A second operating point where c_{O_2} < 25 mg/L (the concentration above which the microalgae are inhibited) was considered for linearization. For this point the combination of gas flows is $Q_{in}^{N_2}$ = 30 mL/min and $Q_{in}^{CO_2}$ = 1.64 mL/min.

$$\Lambda_{c_{O_2}=20.3}^{\text{pH}=7.5} = \begin{bmatrix} 0.9884 & 0.0116 \\ 0.0116 & 0.9884 \end{bmatrix} \quad (16)$$

It can be seen (15 and 16) that the cross-interactions remain low, the analysis pointing towards decentralized control. Whether the culture is operated above or below the inhibition point (c_{O_2} = 25 mg/L), the system is not influenced by the decrease of biomass. The same effect is obtained by variating D or q_0.

Two more points with pHs outside the optimal value have been considered for linearization. $Q_{in}^{N_2}$ = 20 mL/min and $Q_{in}^{CO_2}$ = 9.8 mL/min will shift the pH towards lower values, presenting consistent cross-interactions as it can be seen above:

$$\Lambda_{c_{O_2}=17.6}^{\text{pH}=6.5} = \begin{bmatrix} 0.7098 & 0.2902 \\ 0.2902 & 0.7098 \end{bmatrix} \quad (17)$$

Shifting the pH to the right ($Q_{in}^{N_2}$ = 20 mL/min and $Q_{in}^{CO_2}$ = 0.413 mL/min), the cross-interactions are lower:

$$\Lambda_{c_{O_2}=20.9}^{\text{pH}=8.5} = \begin{bmatrix} 0.8825 & 0.1175 \\ 0.1175 & 0.8825 \end{bmatrix} \quad (18)$$

It can be concluded that the pH control loop will be strongly influenced by the c_{O_2} control loop mostly at low pHs where the decentralized control may give unsatisfactory results. Simulations with $f_{\text{pH}} = 1$ (i.e. the pH doesn't influence the growth rate) revealed that there are no cross-interactions at higher pHs than the optimal pH, but only at lower pHs. Thus, the cross-interactions become consistent mainly when the ratio between $Q_{in}^{CO_2}$ and $Q_{in}^{N_2}$ becomes higher (17). On the other hand, the c_{O_2} control loop will not suffer much because the N_2 flow rate is higher that the CO_2 flow rate in most cases.

IV. Controller Design

The global photoautotrophic growth model was implemented in Simulink, in the first instance to be linearized for the RGA analysis and second, to design and test the control system.

Conventional PID/PI controllers were added to each cannel (Fig. 4) because they are easier to be implemented on an experimental laboratory photobioreactor. The tuning of the controllers was done using the trial and error method, aiming stability and good set-point tracking properties characterized by zero steady-state error and an overshoot below 3% when a step change is introduced in the set-point. An ideal PID controller was added for the pH loop (the derivative action was introduced because the system behaves as a second order system in open loop). Based on the IMC tuning method the parameters of the controller (i.e. $\text{PID}(s) = \text{P}(1 + \text{Is}^{-1} + D(1 + \text{s}^{-1})^{-1})$ were set as follows: $\text{P} = -0.1$, $\text{I} = 1/4$ and $\text{D} = 1/2$. For the dissolved oxygen loop, a PI controller was selected because it behaves as a first order system. Its parameters were found in the same way as the parameters of the pH controller: $\text{P} = -10^{-4}$ and $\text{I} = 1$.

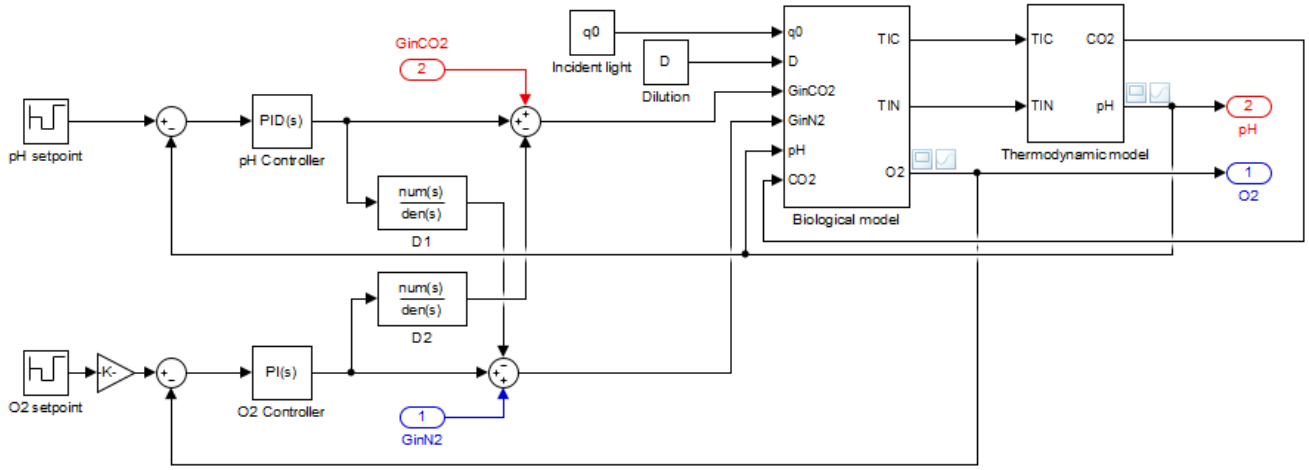

Fig. 4. The Simulink control scheme of the PBR with the interconnections between the biological and thermodynamic sub-model

Based on the RGA analysis from the previous section, a decoupling structure with feedforward controllers was designed according to the following method. First order linear models were identified on the step responses for the direct and cross channels. First order models were preferred for the ease of practical implementation on a laboratory PBR, even though second order models (at least for the pH loop) would be more accurate.

Based on the resulted transfer matrix of the process,

$$H_p(s) = \begin{bmatrix} H_{p11}(s) & H_{p12}(s) \\ H_{p21}(s) & H_{p22}(s) \end{bmatrix}$$

the transfer matrix of the decoupling system is calculated,

$$D(s) = \begin{bmatrix} 1 & D_1(s) \\ D_2(s) & 1 \end{bmatrix}.$$

The transfer matrix of the decoupled system is $H_{dec}(s) = H_p(s) \cdot D(s)$, and imposing

$$H_{dec}(s) = \begin{bmatrix} H_{dec11}(s) & 0 \\ 0 & H_{dec22}(s) \end{bmatrix},$$

to have zero contribution from the secondary channels, the transfer functions for decoupling will be obtained with:

$$D_1(s) = -H_{p12}(s)/H_{p11}(s) \quad (19)$$

$$D_2(s) = -H_{p21}(s)/H_{p22}(s) \quad (20)$$

The resulted transfer functions are:

$$D_1(s) = \frac{0.0049 \cdot s + 0.0491}{s + 0.1818} \quad (21)$$

$$D_2(s) = \frac{0.00546 \cdot s + 0.000273}{s + 0.25} \quad (22)$$

The PID/PI controllers, along with the decoupling system were implemented in Simulink and tested on the nonlinear photoautotrophic growth model as seen in Fig. 4.

V. Simulation Results

To investigate the efficiency of the two controllers and of the feedforward action the process was simulated on 300 hours at a constant dissolved oxygen concentration (Fig. 5).

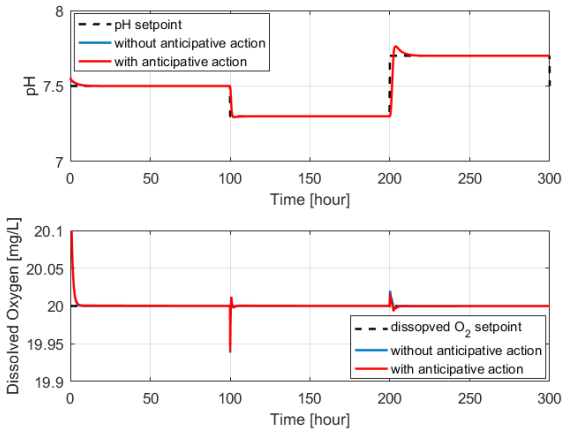

Fig. 5 Simultaneous control of pH and DO. Influence of pH control loop over the DO control loop

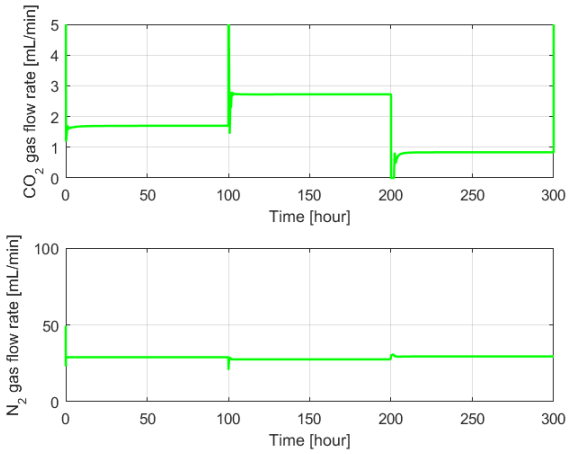

Fig. 6. Input variable evolution during the simultaneous control of pH and DO - pH steps

As expected, the pH loop doesn't influence much the c_{O_2} control loop as it can be seen in Fig. 5, where a sequence of steps was imposed to the pH each 100 hour.

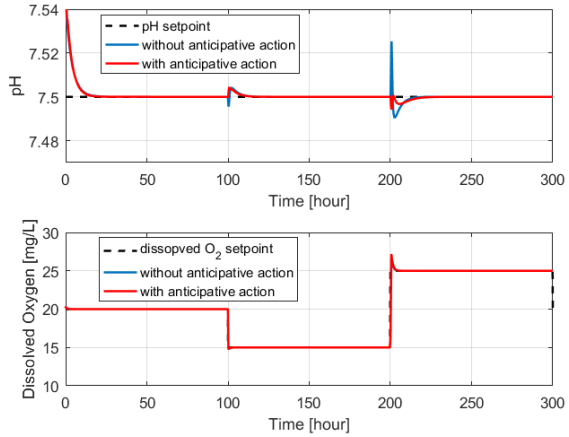

Fig. 7 Simultaneous control of pH and DO. Influence of DO control loop over the pH control loop

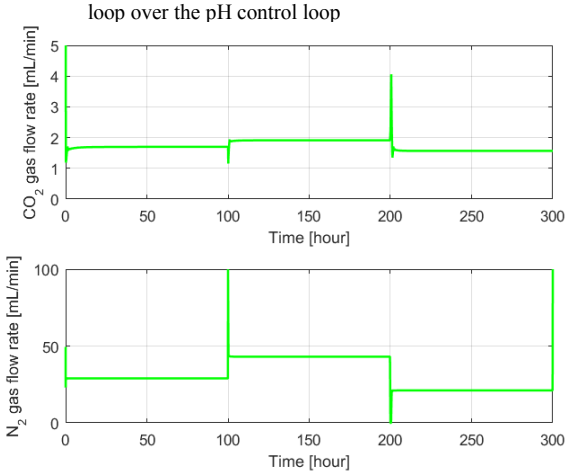

Fig. 8. Input variable evolution during the simultaneous control of pH and DO - DO steps

Steps were imposed to the c_{O_2} to observe its influence on the pH. The disturbances are stronger on this case, the pH being sensitive to c_{O_2} change. The efficiency of the feedforward action can be observed in this case (red line)

compared to the system with nothing more than linear controllers (blue line). Fig. 7 shows simulation results that confirms the efficiency of the decoupling structure based on feedforward controllers.

The system would work well with only one feedforward action, namely $D_2(s)$, which would account only the effect of the DO over the pH. This can be explained also through the fact that the CO_2 gas flowrate is considerably lower than the N_2 gas flowrate (in extreme cases can be over 100 times lower). The decoupling structure would be a good addition on an experimental PBR and could minimize the eventual unsatisfactory control results given by the misfit between the mathematical model and the process and eventually the poorly chosen parameters of the controller.

CONCLUSIONS

This work investigates simultaneous control of pH and dissolved oxygen concentration in a closed photobioreactor, using linear technics. This study was performed in simulation and was based on a previous dynamic model able to describe the complexity of this multivariable biological process. This model has been validated on a lab scale setup, used to investigate dynamic behavior of the microalgae photosynthesis and respiration. Controlling dissolved oxygen concentration at different levels is of crucial importance; at the same time, pH has to be regulated at the optimum. This study illustrates that the use of individual conventional PIDs could be unsatisfactory because of existing interactions and proposes a feedforward compensation improving control performances.

ACKNOWLEDGMENT

The authors from University of Nantes would like to thank Pays de la Loire Region who founded part of this work by Regional Project AMI "Projet AMI - Atlantic MIcroalgae - Pôle Microalgues de la Région des Pays de la Loire (http://www.atlanticmicroalgae.univ-nantes.fr/). Part of this work has been supported by Cajamar Foundation and partially funded by the following projects: DPI2014-55932-C2-1-R, DPI2014-56364-C2-1-R and DPI2012-31303 (financed by the Spanish Ministry of Economy and Competitiveness and EU-ERDF funds); Controlcrop P10-TEP-6174 (financed by the Consejería de Economía, Innovación y Ciencia de la Junta de Andalucía); CENIT VIDA (financed by the Spanish Ministry of Economy and Competitiveness and CDTI funds); and the UNED through a postdoctoral scholarship.

REFERENCES

[1] S.-K. Kim (Ed.), Handbook of Marine Microalgae: Biotechnology Advances, Academic Press, 2015.

[2] P. Spolaore, C. Joannis-Cassan, E. Duran, A. Isambert, Commercial applications of microalgae, J. Biosci. Bioengin., vol 101, pp. 87–96, 2006.

[3] Y. Chisti, Biodiesel from microalgae, Biotechno. Adv., vol. 25, 294–306, 2007.

[4] A. Pandey, Biofuels: Alternative Feedstocks and Conversion Processes Academic Press, 2011.

[5] Jiang, L., Luo, S., Fan, X., Yang, Z., Guo, R.: Biomass and lipid production of marine microalgae using municipal wastewater and high concentration of CO2. Applied energy, 88, pp. 3336–3341, 2011.

[6] M.K. Lam, K.T. Lee, A.R. Mohamed, Current status and challenges on microalgae-based carbon capture, Int. J. Greenhouse Gas Contr., vol. 10, pp. 456–469, 2012

[7] J.R. Benemann, CO_2 mitigation with microalgae systems, Energy Conversion and Management, Vol. 38, Supp., 1997, pp. S475-S479

[8] J. Pruvost, F. Le Borgne, A. Artu, J. Legrand, Development of a thin-film solar photobioreactor with high biomass volumetric productivity (AlgoFilm©) based on process intensification principles, Algal Research, Vol. 21, 2017, Pages 120-137

[9] O. Bernard, Hurdles and challenges for modelling and control of microalgae for CO2 mitigation and biofuel production, J. Process Contr., vol. 21, pp. 1378–1389, 2011

[10] S. Tebbani, F. Lopes, R. Filali, D. Dumur, D. Pareau, CO2 Biofixation by Microalgae: Modeling, estimation and control. ISTE – Wiley, 2014.

[11] L. Mailleret, O. Bernard, J.P. Steyer, Nonlinear adaptive control for bioreactors with unknown kinetics. Automatica, vol. 40, pp. 1379–1385, 2004.

[12] G.A. Ifrim, M. Titica, M. Barbu, L. Boillereaux, G. Cogne, S. Caraman, J. Legrand, Multivariable feedback linearizing control of *Chlamydomonas reinhardtii* photoautotrophic growth process in a torus photobioreactor, Chem. Engin. J., vol. 218, pp. 191–203, 2013

[13] I. Fernández, M. Berenguel, J.L. Guzmán, F.G. Acién, G.A. de Andrade, D.J. Pagano, Hierarchical control for microalgae biomass production in photobiorreactors, Control Engineering Practice, Vol. 54, 2016, Pages 246-255

[14] M. Berenguel, F. Rodríguez, F.G. Acién, J.L. García, Model predictive control of pH in tubular photobioreactors, Journal of Process Control, Volume 14, Issue 4, 2004, Pages 377-387

[15] A. Pawlowski, J.L. Mendoza, J.L. Guzmán, M. Berenguel, F.G. Acién, S. Dormido, Selective pH and dissolved oxygen control strategy for a raceway reactor within an event-based approach, Control Engineering Practice, Vol. 44, 2015, Pp. 209-218.

[16] Raso, Sayam, Bernard van Genugten, Marian Vermuë, et René H. Wijffels. 2012. « Effect of oxygen concentration on the growth of Nannochloropsis sp. at low light intensity ». *Journal of Applied Phycology* 24 (4):863‑71

[17] Sousa, Claudia, Ana Compadre, Marian H. Vermuë, et Rene H. Wijffels. 2013. Effect of oxygen at low and high light intensities on the growth of Neochloris oleoabundans. *Algal Research* 2 (2):122‑26.

[18] Costache, T. A., F. Gabriel Acién Fernández, M. M. Morales, J. M. Fernández-Sevilla, I. Stamatin, et E. Molina. 2013. « Comprehensive Model of Microalgae Photosynthesis Rate as a Function of Culture Conditions in Photobioreactors ». *Applied Microbiology and Biotechnology* 97 (17):7627‑37.

[19] Fouchard, S. , Pruvost, J. , Degrenne, B. , Titica, M. and Legrand, J. (2009), Kinetic modeling of light limitation and sulfur deprivation effects in the induction of hydrogen production with *Chlamydomonas reinhardtii*: Part I. Model development and parameter identification. Biotechnol. Bioeng., 102: 232-245.

[20] G.A. Ifrim, M. Titica, G. Cogne, L. Boillereaux, S. Caraman, J. Legrand, Dynamic pH model for autotrophic growth of microalgae in a photobioreactor: A tool for monitoring and control purposes, *AIChE Journal*, 60: 585–599, 2014

[21] Souliès, Antoine, Jack Legrand, Hélène Marec, Jérémy Pruvost, Cathy Castelain, Teodor Burghelea, et Jean-François Cornet. 2016. « Investigation and Modeling of the Effects of Light Spectrum and Incident Angle on the Growth of Chlorella Vulgaris in Photobioreactors ». *Biotechnology Progress* 32 (2):247 ‑ 61. https://doi.org/10.1002/btpr.2244.

[22] Molina Grima, E., F. G. Acién Fernández, F. García Camacho, et Yusuf Chisti. 1999. « Photobioreactors: light regime, mass transfer, and scaleup ». *Journal of Biotechnology*, Biotechnological Aspects of Marine Sponges, 70 (1):231‑47.

[23] E. Bristol, On a new measure of interaction for multivariable process control. IEEE Transactions on Automatic Control. 1966; 11(1):133-134.